A PHOTOMETRIC AND SPECTROSCOPIC STUDY OF THE CATACLYSMIC VARIABLE SX LEONIS MINORIS IN QUIESCENCE AND SUPEROUTBURST[1]

R. Mark Wagner,[2] John R. Thorstensen,[3] R. K. Honeycutt,[4] S. B. Howell,[5] R. H. Kaitchuck,[6] T. J. Kreidl,[7] J. W. Robertson,[4] E. M. Sion,[8] and S. G. Starrfield[9]

ABSTRACT

We present CCD imaging, CCD photometry on long and short timescales, and time-resolved spectroscopy of SX LMi, a new SU Ursae Majoris type dwarf nova. The quiescent optical spectrum shows broad double-peaked Balmer, He I, and He II emission lines, similar to other quiescent dwarf novae. Absorption lines from a late-type secondary are not detected. Time-resolved spectra obtained in quiescence reveal radial velocity variations of the Balmer emission lines on a period of 0.06717 ± 0.00011 days, or 96.72 ± 0.16 minutes, with only a slight possibility of a daily cycle-count error. Optical photometry obtained between 1987 and 1991 shows flickering with a peak-to-peak amplitude of $\simeq 0.18$ mag. The binary orbital period can sometimes be seen in the photometric record. Long-term photometric monitoring by Indiana University's robotic telescope RoboScope for a 3 year period between 1992 October and 1995 June shows seven well-defined outbursts and marginally detects a few others. The outburst interval varies between 34 and 64 days. During the 1994 December outburst, optical photometric observations show that SX LMi exhibited superhumps with a period of 0.06893 ± 0.00012 days, which is $2.6\% \pm 0.2\%$ longer than the orbital period, as expected for a normal SU UMa star at this period. Spectra obtained during superoutburst show dramatic variations in the emission-line profiles on timescales of 10 minutes. Profile fits indicate that underlying absorption contributes to the shape of the Balmer emission-line profiles during superoutburst as in other dwarf novae in outburst or superoutburst. Direct images in good seeing show a ~ 19 mag companion star $1\farcs95$ from SX LMi.

Key words: binaries: general — stars: individual (SX Leonis Minoris) — stars: variables: other

1. INTRODUCTION

Cataclysmic variables (CVs) are close binary systems in which matter is transferred onto a white dwarf from a Roche lobe–filling secondary star. (For a recent summary describing the observations, models, and theoretical aspects of the entirety of cataclysmic variables, see the excellent book by Warner 1995.) The dwarf novae form a subclass of the CVs characterized by outbursts with amplitudes of 2–8 mag lasting for days to weeks. The mean interval between outbursts varies widely, from ~ 10 to 10^4 days. The SU Ursae Majoris stars are a subgroup of the dwarf novae characterized by ordinary outbursts and occasional brighter and longer "superoutbursts"; their orbital periods are generally ≤ 2 hr. During superoutburst, SU UMa stars show periodic oscillations in brightness, called "superhumps," with amplitudes of a few tenths of a magnitude but periods a few percent *longer* than the orbital period. The superhumps are widely thought to originate in a precessing elliptical accretion disk (Molnar & Kobulnicky 1992; Osaki 1996).

Here we describe photometric and spectroscopic observations of SX LMi (originally called CBS 31), obtained during quiescence and superoutburst. Wagner et al. (1988) identified SX LMi as a new cataclysmic variable during follow-up spectroscopy of the Case Low-Dispersion Northern Sky Survey (Sanduleak & Pesch 1984).

2. IMAGING AND ASTROMETRY

During our photometric and spectroscopic study of SX LMi, we noted the presence of a faint star near SX LMi both on direct CCD frames and guiding TVs. Under good seeing conditions on 1996 April 9.29 UT, we obtained four *V*-band dithered 180 s CCD direct exposures using the 2.4 m Hiltner Telescope at Michigan-Dartmouth-MIT (MDM) Observatory and a "piggyback" direct camera that had been added to support a monitoring program (Fig. 1). E. E. Falco later kindly obtained brief exposures with a wider field direct camera. We measured the pixel position and the relative brightness of this star using DAOPHOT and determined an astrometric position from four nearby *Hubble Space Telescope* (*HST*) guide stars on the widest field frame. The tangent-plane least-squares fit yielded an rms residual of $0\farcs34$ for the *HST* guide stars and a celestial position $\alpha = 10^{\rm h}54^{\rm m}30\fs455$, $\delta = 30\arcdeg06\arcmin10\farcs09$ for SX LMi itself. These are equinox J2000.0 and epoch 1996.3.

The companion star is $1\farcs95$ distant in position angle 192°. We did not observe standard stars, but the companion is

---

[2] Department of Astronomy, Ohio State University, 174 West 18th Avenue, Columbus, OH 43210. Current address: Lowell Observatory, 1400 West Mars Hill Road, Flagstaff, AZ 86001.

[3] Department of Physics and Astronomy, 6127 Wilder Laboratory, Dartmouth College, Hanover, NH 03755-3528.

[4] Department of Astronomy, Indiana University, Bloomington, IN 47405.

[5] Department of Physics and Astronomy, University of Wyoming, P.O. Box 3905, University Station, Laramie, WY 82071.

[6] Department of Physics and Astronomy, Ball State University, Muncie, IN 47306.

[7] Computing Technology Services, Northern Arizona University, Box 5100, Flagstaff, AZ 86011.

[8] Department of Astronomy and Astrophysics, Villanova University, Villanova, PA 19085.

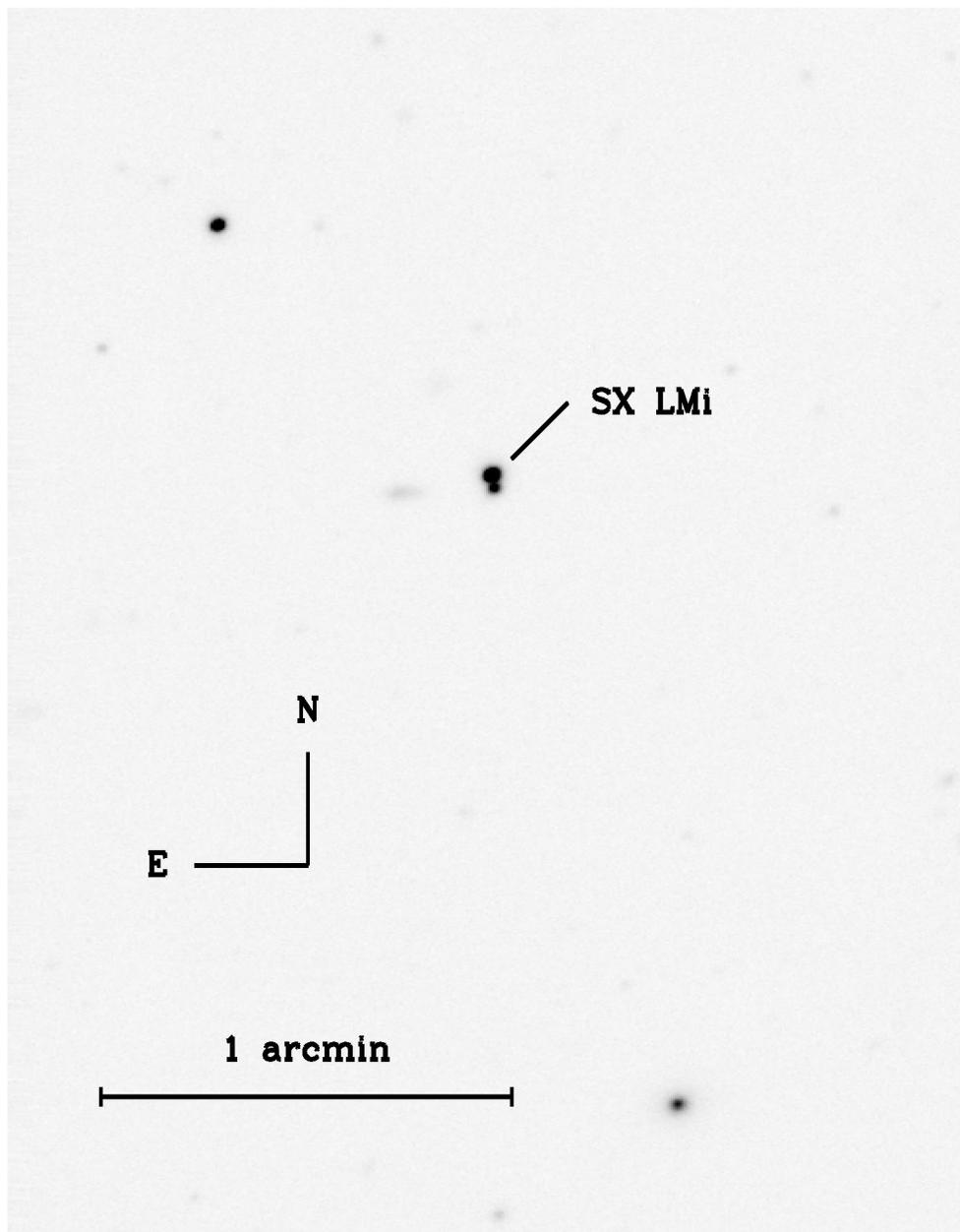[9] Department of Physics and Astronomy, Arizona State University, Tempe, AZ 85287.

FIG. 1.—V-band identification chart for SX LMi. North is to the top and east to the left. The field of view is approximately $2\overset{.}{.}3 \times 3\overset{.}{.}0$. Note the faint companion adjacent to SX LMi.

0.95 V mag fainter than the star 54″ northeast of SX LMi, and 1.60 V mag fainter than SX LMi itself at the time of our exposure. If the quiescent magnitude of SX LMi is $V \simeq 17.4$ mag, as measured by RoboScope (see below), then the companion would be at $V = 19.0$ mag and the star 54″ northeast of SX LMi would be at $V = 18.1$ mag. Examination of the Palomar Observatory Sky Survey (POSS) E print shows a southern elongation of the image of SX LMi corresponding to the companion, but at a position angle of 170°–175°. The image of SX LMi on the POSS O print is circular and does not reveal the companion, which suggests that it is quite red in color.

The difference in position angle between the two epochs, ~42 years apart, indicates substantial relative motion between SX LMi and the close companion, which might result from their relative proper motions or perhaps orbital

motion about a common center of mass. If the companion star's proper motion or radial velocity shows it to be physically associated with SX LMi in a wide resolved binary system, it offers a possibility of determining the spectroscopic parallax and, hence, distance to SX LMi based on the spectral type of the companion. We also note the presence of a ~19th magnitude star $2\overset{s}{.}3$ west and 4″.3 south of SX LMi that is visible on the POSS E print but absent on the POSS O print and our V-band CCD frame (Fig. 1). The nature of this object is unclear.

3. LONG-TERM PHOTOMETRIC BEHAVIOR

Three years of CCD photometry of SX LMi were obtained using RoboScope, the Indiana University unattended photometric system (Honeycutt et al. 1990; Honeycutt & Turner 1992) and are shown in Figure 2.
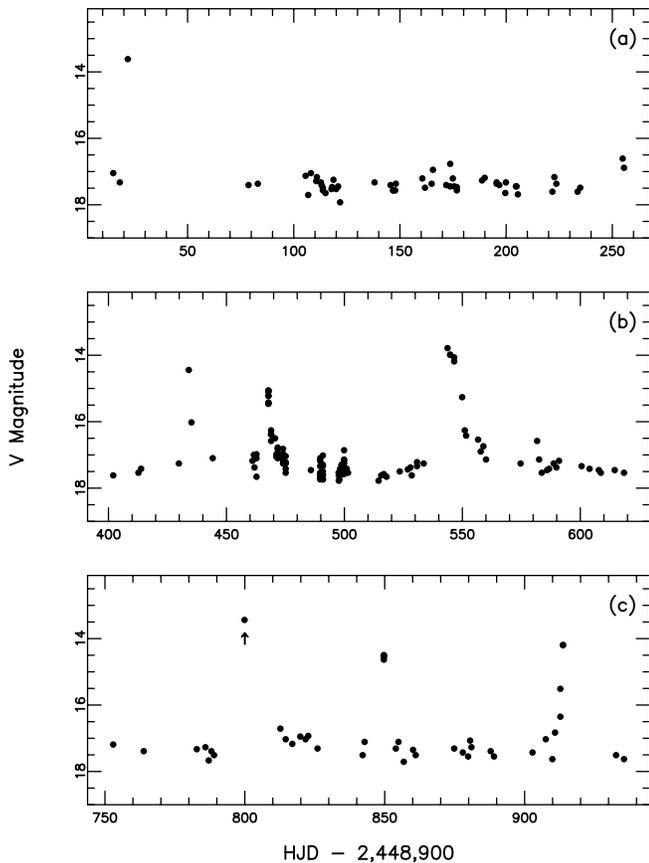
FIG. 2.—RoboScope light curves of SX LMi. (*a*) 1992 October 19 through 1993 June 16; (*b*) 1993 November 10 through 1994 June 15; (*c*) 1994 October 27 through 1995 April 28. In (*c*), the 1994 December super-outburst is indicated by an arrow. Typical errors in the differential photometry are 0.01 mag in outburst and 0.05 mag in quiescence.

Usually a single exposure of SX LMi was obtained each clear night, resulting in 217 usable data points on 141 separate nights during the interval 1992 October 19 (UT) to 1995 April 28. For a few weeks in the winter of 1994, the frequency of observations was increased to an average of seven exposures each usable night. The data were reduced using the method of inhomogeneous ensemble photometry (Honeycutt 1992) and nine comparison stars. Typical errors vary from 0.01 mag during outburst to 0.05 mag in quiescence. The zero point was established to an accuracy of 0.01–0.02 mag using the secondary standards of Henden & Honeycutt (1995).

In Figures 2*a*–2*c*, we see seven well-defined outbursts (at JD − 2,440,000 = 8,922, 9,334, 9,368, 9,444, 9,700, 9,750, and 9,814) and marginally detect a few others. The outbursts typically have amplitudes of 3.5 mag. Most outbursts are poorly sampled, but we note that the outbursts at 9,368 and at 9,444 have resolved *e*-folding decay times of ∼1 and ∼3 days, respectively, while the outburst at 9,814 has a resolved *e*-folding rise time of about 1 day. The outburst interval appears to vary between 34 days (JD 9,368–9,334) and 64 days (note the relatively well sampled interval between JD 9,750 and 9,814). Figure 2*b* shows the data for a 3 month interval when the density of the data points was increased. We note that the mean quiescence brightness falls slowly after outburst, and rises slowly before outburst. These trends are superposed on about 0.7 mag of variation within a night.

4. AVERAGE SPECTRUM IN QUIESCENCE

The discovery spectrum of SX LMi as shown in Wagner et al. (1988) and obtained on 1986 March 8 is dominated by strong emission lines of hydrogen, He I $\lambda5876$, $\lambda5015$, $\lambda4922$, and $\lambda4471$, and weaker He II $\lambda4686$ on a blue continuum.
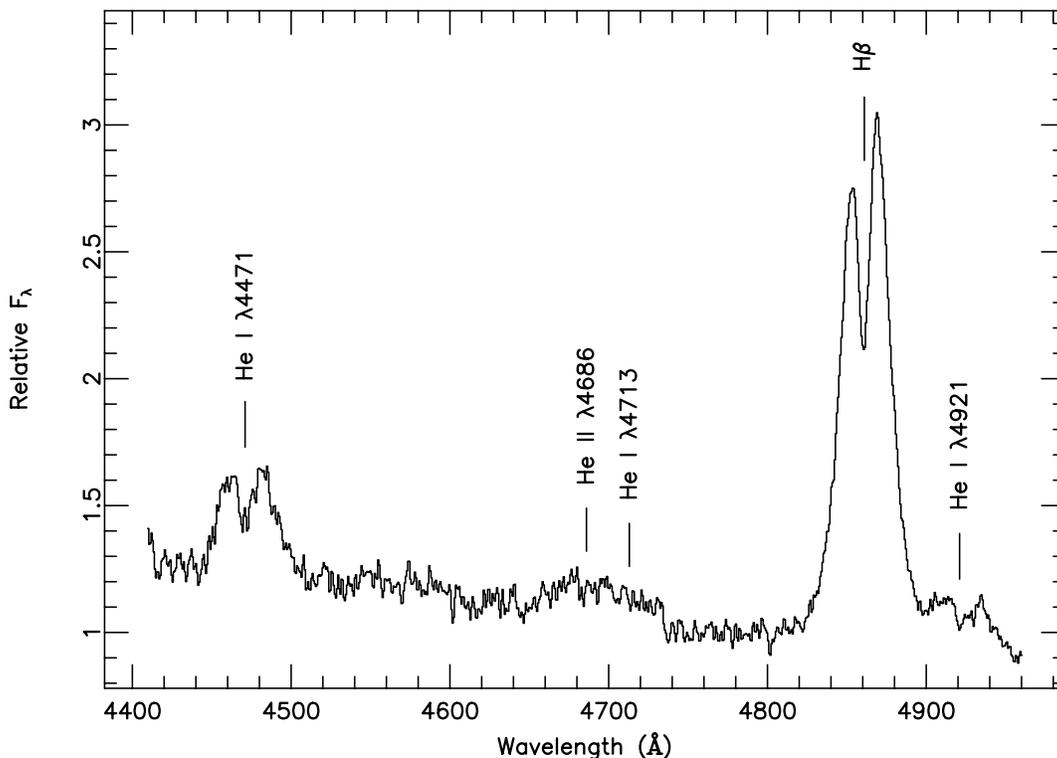

FIG. 3.—Spectrum of SX LMi obtained at the MMT on 1991 January 16 at a spectral resolution of 2.5 Å as part of a radial velocity study of the system. The Hβ profile is double-peaked but asymmetric to the red.
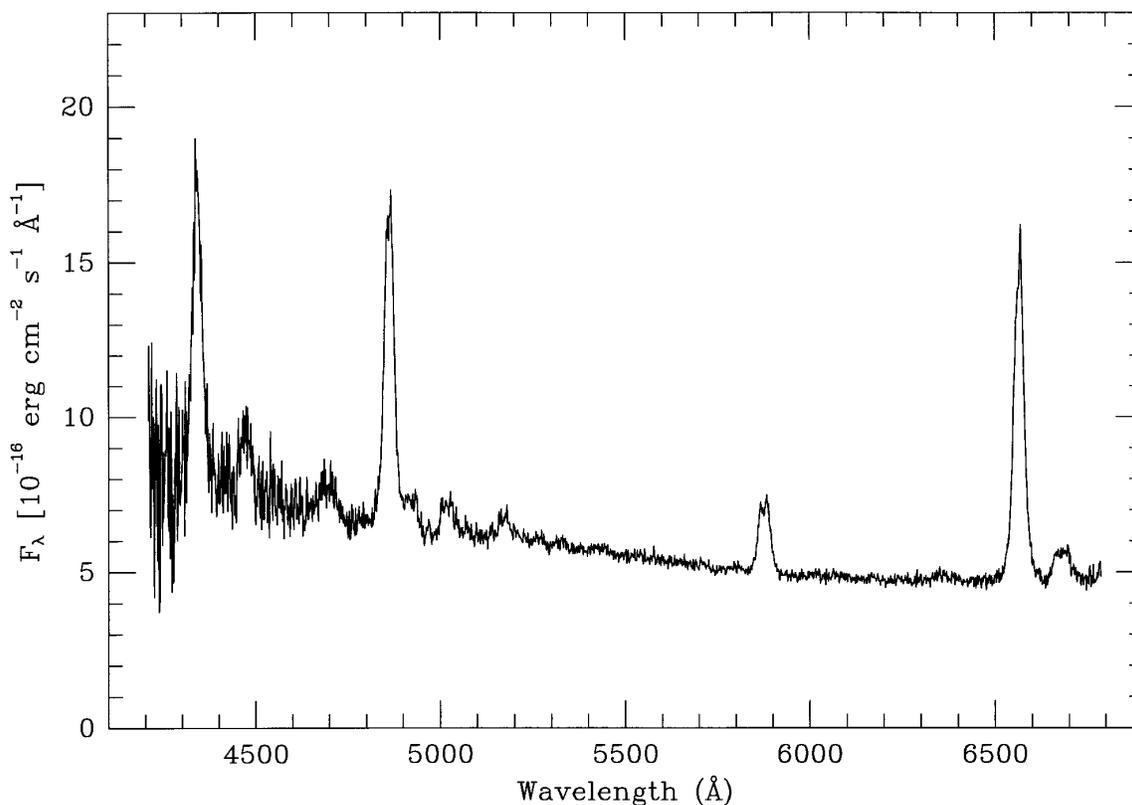
FIG. 4.—Mean spectrum of SX LMi with a spectral resolution of about 3 Å obtained 1996 April with the MDM 2.4 m telescope. The flux scale is unreliable because of clouds and losses at the spectrograph slit.

The profiles are distinctly double-peaked, with FWHM $\simeq$ 2200 km s^{-1}. The FWZI of Hβ emission is 4300 km s^{-1}, and the Balmer continuum is prominent in emission. The flux level of the spectrum corresponds to $V = 17.3$ mag and is consistent with SX LMi in quiescence as indicated by the RoboScope photometry (Fig. 2). The discovery spectrum is similar to those of other dwarf novae in quiescence. The equivalent widths of the prominent emission lines are Hβ, 73 Å; Hγ, 55 Å; He I λ4471, 16 Å; and He II λ4686, 7 Å.

Figure 3 shows a spectrum of SX LMi from 4400 to 4960 Å at a spectral resolution $\Delta\lambda \simeq 2.5$ Å obtained 1991 January 16 at the 4.5 m Multiple Mirror Telescope (MMT) with the red channel spectrograph, 1200 line mm^{-1} grating, and 1″25 slit. Simultaneous CCD photometry (see below) yields $V = 16.8$, somewhat brighter than its typical quiescent magnitude of 17.4. The composite spectrum was formed by averaging the 14 individual spectra in our radial velocity study (see below), after shifting to the rest frame of the emission lines. The average spectrum was then normalized to the level of the continuum at 4800 Å. Prominent Hβ and He I λ4471 emission lines appear superposed on a blue continuum. He II λ4686 is broad and weak. The line profiles are double-peaked, but the red peaks are brighter than the blue. This is especially evident in Hβ but less so in the He I profiles. The measured emission equivalent widths are Hβ, 64 Å; He I λ4471, 11 Å; He II λ4686, 9 Å and are consistent with our initial observations listed above. The FWZI of Hβ emission is 4800 km s^{-1}.

Figure 4 shows the average of 38 spectra obtained using the MDM Observatory 2.4 m Hiltner Telescope and the

Modular Spectrograph. A Loral 2048^2 unthinned CCD and 600 line mm^{-1} grating yielded coverage from 4200 to 6780 Å at a dispersion of 1.27 Å pixel^{-1} and a spectral resolution of $\Delta\lambda \sim 3$ Å. The observing protocol emphasized maintenance of an accurate wavelength scale for velocity measurements, and night-sky lines were stable within a few km s^{-1} in the reduced data. The total integration time of 5.1 hr spanned five nights in 1996 April; the data were reduced using procedures in IRAF. The data shown have been flux-calibrated, but the vertical scale is untrustworthy because of unknown slit losses; even the continuum may be slightly distorted because of a poorly understood instrumental problem (radial velocity measurements are unaffected). There is He II λ4686 emission with $\sim$ 12 Å EW, and the Hβ and He I λ5876 lines show slight doubling (no velocity shifts were applied before adding). The equivalent width of Hβ is $\sim$ 52 Å, and that of Hα is 83 Å; Hα has an FWHM of 1500 km s^{-1} and an FWZI of 4300 km s^{-1}. The MDM spectrum and equivalent widths appear consistent with those described above and also shown by Szkody & Howell (1992).

5. SHORT-TIMESCALE LIGHT CURVES

On 1987 February 6, we obtained V-band photometry using the 1.8 m Perkins Telescope of the Ohio Wesleyan and Ohio State Universities at the Lowell Observatory and the Lowell RCA CCD camera. A 4:1 focal reduction camera and the extraction of a 256 × 256 pixel image centered near SX LMi yielded a 3′ × 3′ field at 0″8 pixel^{-1}. Integration times were generally 3 minutes, with a dead time of $\sim$ 30 s. After bias and flat-field correction, we performed differential
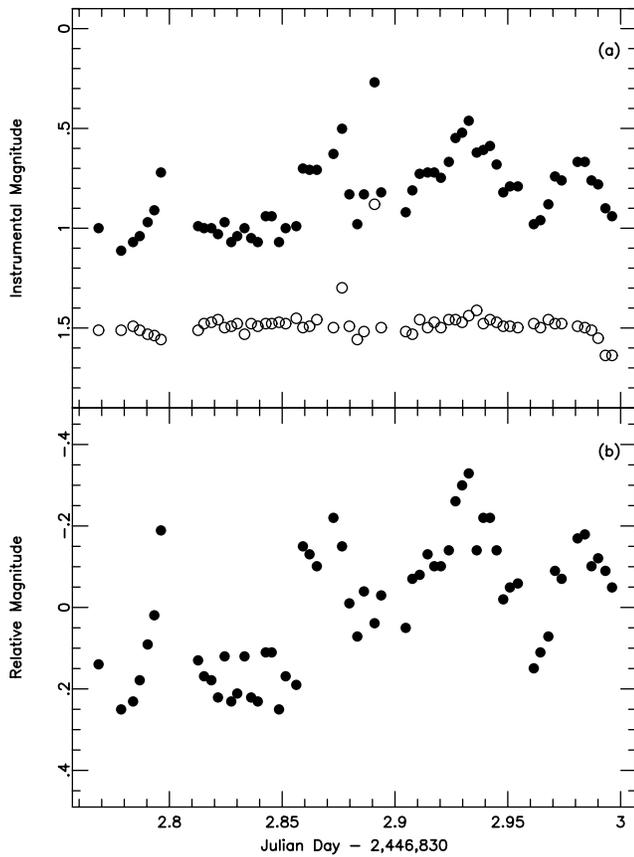
FIG. 5.—(a) Observed magnitudes of SX LMi (*filled circles*) and a comparison star (*open circles*). Note the constancy of the comparison star magnitudes during the night relative to SX LMi. (b) Differential light curve of SX LMi on 6 February 1987. Note the flares on three occasions that are separated by about 1.5 hr.

aperture photometry using the 18.1 mag star 54" northeast of SX LMi as the comparison (see Fig. 1). This was the only usable comparison in the small field of view. No absolute calibration was attempted; however, the magnitude difference between SX LMi and the comparison star at the time of our observations was consistent with SX LMi being in quiescence.

Figure 5a shows the photometry of SX LMi (*filled circles*) and the comparison star (*open circles*). Note the constancy of the comparison star; ignoring two discrepant points (TJD 2.8765 and 2.8907) yields a standard deviation of the comparison star of only 0.04 mag. Because there was no check star, we could not estimate the accuracy of the differential light curve, using (for example) the technique outlined by Howell, Mitchell, & Warnock (1988); even so, the scatter of the comparison star instrumental magnitudes (which is not differential) sets an upper limit to the uncertainties in the differential magnitudes. From differential photometry of comparably faint stars in other fields, in which check stars were available, we estimate that the differential light curve of SX LMi is accurate to better than 1%. Figure 5b shows the differential light curve. SX LMi brightens on at least three occasions, each separated by about 1.5 hr, but the form of each brightening is slightly different. Changes in brightness of 0.3 mag on a timescale of a few minutes are also apparent in Figure 5b, as is a general upward trend of about 0.2 mag during the observations.

We searched the differential light curve for periodic variations using two different techniques, and we show the results in Figure 6. First, sine functions (Fig. 6a) with trial periods between 0.05 and 3 hr were fitted to the data, yielding a significant decrease in the mean square residual for trial periods of 1.5 ± 0.2 hr. Second, the phase dispersion minimization method of Stellingwerf (1978), which makes
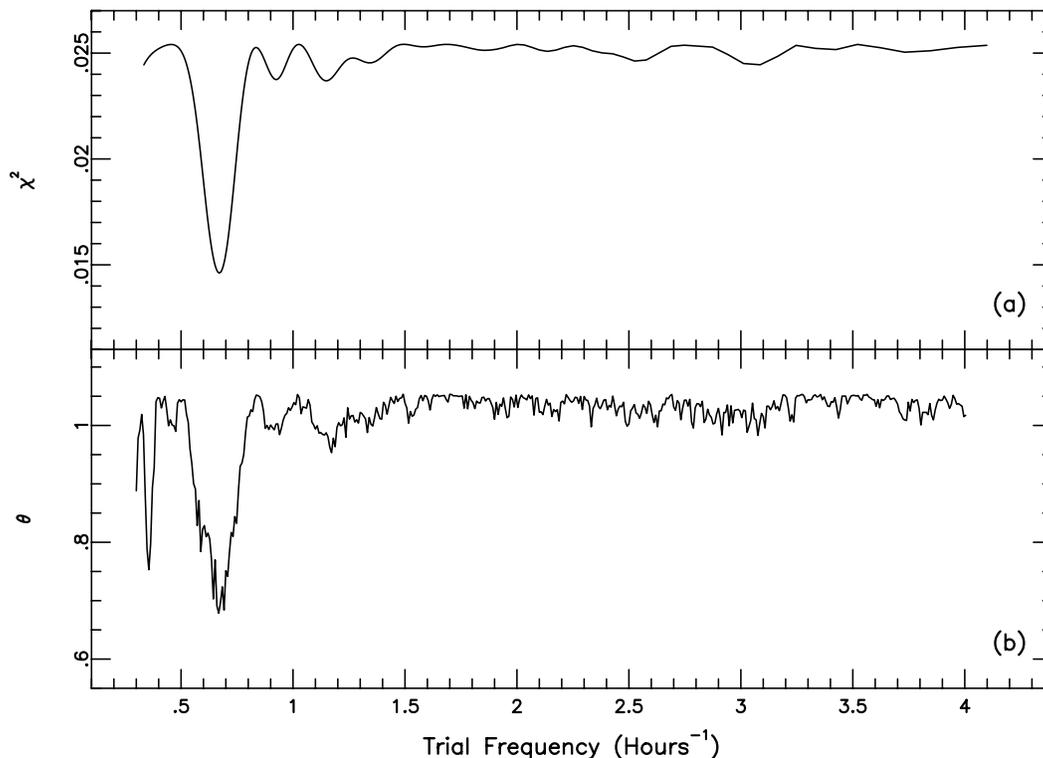

FIG. 6.—Period search of the data in Fig. 5 based on (a) a sine function with trial periods between 0.05 and 3 hr and (b) the phase dispersion minimization method of Stellingwerf (1978). A period of 1.492 hr, or 0.062 days, was found in both searches.
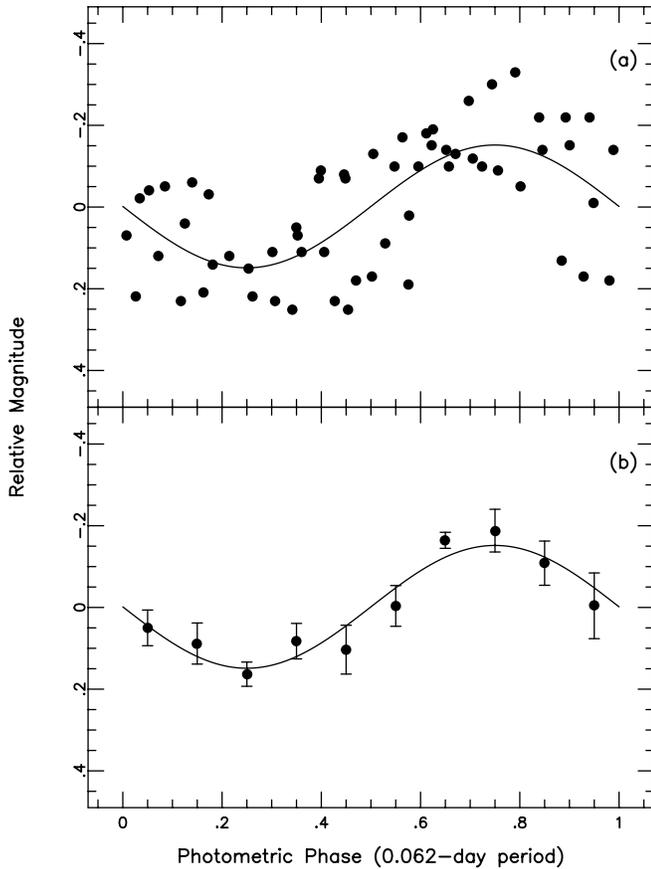
FIG. 7.—(a) Data from Fig. 5b phased on the 1.492 hr period, and (b) data averaged in 10 phase bins. The light curve is nearly sinusoidal on average.

FIG. 8.—CCD photometry obtained (a) 1991 January 15 and (b) 1991 January 16 at the Perkins Telescope.

no assumptions concerning the light-curve shape, was used with a (4, 1) binning structure (Fig. 6b). This also yielded a statistically significant 1.5 hr (= 0.062 days) period.

In Figure 7a, we show the data phased on the 0.062 day period, with phase zero corresponding to the time of the first data point (JD 2,446,832.7684). The flickering makes the light curve noisy. Figure 7b shows the data averaged in 10 phase bins; the error bars represent the standard deviation of the mean magnitude in each bin. The mean light curve on the 0.062 day period appears nearly sinusoidal, with a peak-to-peak amplitude of ~0.35 mag.

We obtained additional photometry on 1991 January 15–16 UT (Fig. 8) while SX LMi was in quiescence. The January 16 data were simultaneous with spectroscopy at the MMT and will be discussed below. The Perkins Telescope, the Lowell Observatory Texas Instruments 800^2 CCD camera, and a Johnson V filter were used. The 4:1 focal reduction camera and extraction of a 300 × 300 pixel image yielded a 2′ × 2′ field at 0″.4 pixel^{-1}. The integration time was again 3 minutes and the dead time was again ~30 s. After bias and flat-field correction, we used digital aperture photometry to measure the brightness of SX LMi with respect to the 18.1 mag star 54″ to the northeast. We find $V \simeq 17.5$ mag on January 15 and $V \simeq 16.8$ mag on January 16 for SX LMi.

The light curves (Fig. 8) look similar to those obtained in 1987, except the maxima are much less well defined. These data suggest two photometric maxima per period, in contrast to the 1987 data, which appear nearly sinusoidal with
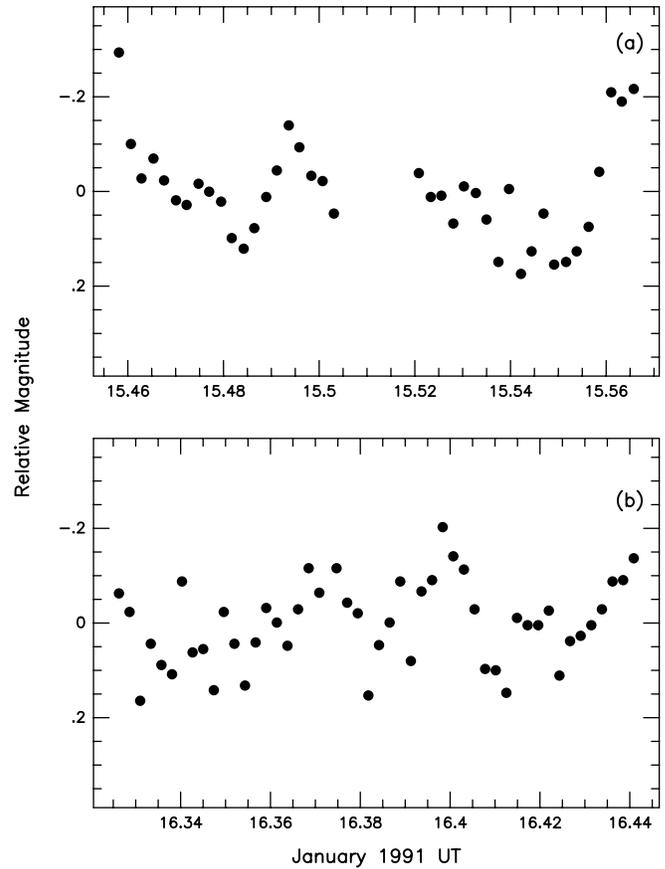
a single maximum. On each night, the maxima are separated by almost exactly half a period, but the flickering makes it difficult to determine the relative phase difference.

6. RADIAL VELOCITY STUDIES

Fourteen 10 minute spectra were obtained with the MMT on the night of 1991 January 16 at minimum light to search for periodic radial velocity variations and other spectroscopic signatures of the candidate period. The details of the equipment are given in § 4 above. Following each spectrum of SX LMi, we observed an HeNeAr comparison lamp for wavelength calibration. The flux-standard star G191-B2B was also observed. We reduced the data with IRAF routines for bias subtraction, flat-fielding, optimal extraction of one-dimensional spectra, wavelength calibration, and conversion to absolute flux. We estimate the internal precision of our radial velocities to be 6 km s^{-1}. Figure 9 shows a montage of the 14 MMT spectra centered on Hβ and displayed in the form of a trailed spectrogram. Radial velocity variations are evident in the two peaks, as well as in the wings of the Hβ line.

Radial velocities were measured by convolving the Hβ emission-line profile with a double-Gaussian mask (Schneider & Young 1980; see also Shafter 1983; Shafter & Szkody 1984). The FWHM of the Gaussian mask was chosen to be 3 Å and thus slightly wider than our nominal spectral resolution. When this approach was applied to these spectra, the dependence of the ratio of the uncertainty in the velocity amplitude and the velocity amplitude, $\sigma(K)/K$, on Gaussian separation showed a flattened para-
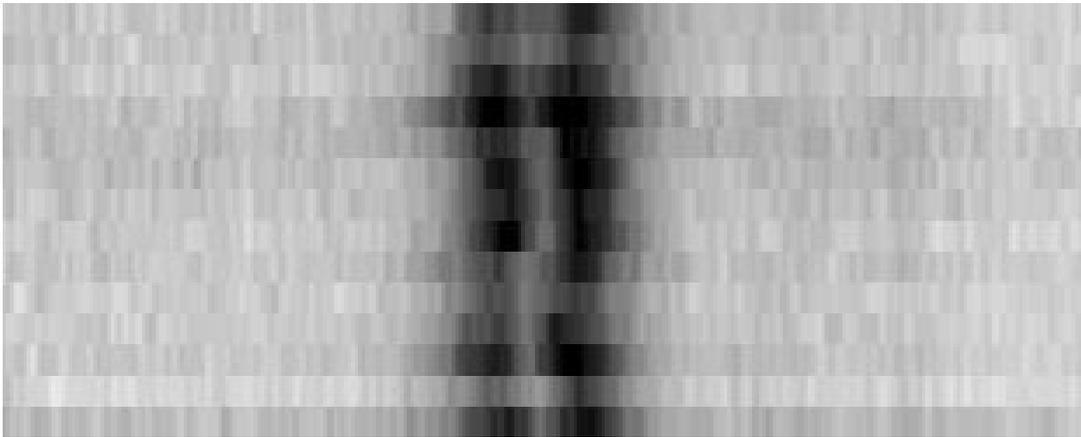
Fig. 9.—Spectra of SX LMi in Hβ obtained at the MMT phased on the photometric period and displayed in the form of a trailed spectrogram. Note the radial velocity variations of the two emission peaks.

bola with a minimum at a separation of 1850 km s^{-1}. For separations between 1400 and 2500 km s^{-1}, K decreased monotonically while $\sigma(K)$ showed a strong parabolic dependence, with a minimum at a separation of 1850 km s^{-1}. This is consistent with the expected behavior; however, we were far from sampling the line profile in the wings, and for larger separations both K and $\sigma(K)$ exhibited strong monotonic increases. One possible explanation for this behavior is that the wings of the line profile are heavily contaminated by a component whose radial velocity variations are significantly out of phase with those of the Hβ-emitting portions of the accretion disk, resulting in very poor fits when the wings are included.

The best-fit circular orbital solution for the Hβ velocities was achieved assuming a Gaussian separation of 1850 km s^{-1}. A least-squares circular orbit fit

$$v(t) = \gamma + K \sin \left[2\pi(t - T_0)/P \right]$$

yielded

$$T_0 = \text{HJD } 2,448,272.792 \pm 0.183 ,$$

$$P = 0.0689 \pm 0.0024 \text{ days} ,$$

$$K = 57 \pm 11 \text{ km s}^{-1} ,$$

$$\gamma = -146 \pm 8 \text{ km s}^{-1} ,$$

$$\sigma = 32.1 \text{ km s}^{-1} ,$$

where σ is the rms residual of the velocities around the fitted sinusoid. The deviant point at phase 0.62 was not included in the orbital solution, though. Here we define phase zero to be inferior conjunction of the primary star, in contrast to the usual notation in which phase zero corresponds to inferior conjunction of the secondary star. In our case, a bright spot normally viewed at phase 0.75 will be seen at phase 0.25.

In Figure 10 (top), we show our Hβ radial velocities with the best-fit circular orbit solution superposed. The solution is acceptable, although there are two extreme deviations from the fitted velocity curve at phases 0.62 and 0.97. However, we note that K as a function of Gaussian separation never showed the expected plateau even though $\sigma(K)/K$ did exhibit the proper dependence for relatively small Gaussian separations that excluded the wings of the line profile. The lower panels of Figure 10 show the photometry

obtained at the Perkins Telescope on January 15 and simultaneously with the MMT radial velocities on January 16. The photometry obtained on both nights exhibits considerable flickering at all orbital phases. The most prominent feature of the light curve on January 15 is a rapid brightening after phase 0.35, reaching a sharp cusp at phase 0.5 and declining quickly thereafter. On January 16, the light curve consists of perhaps two maxima separated by about
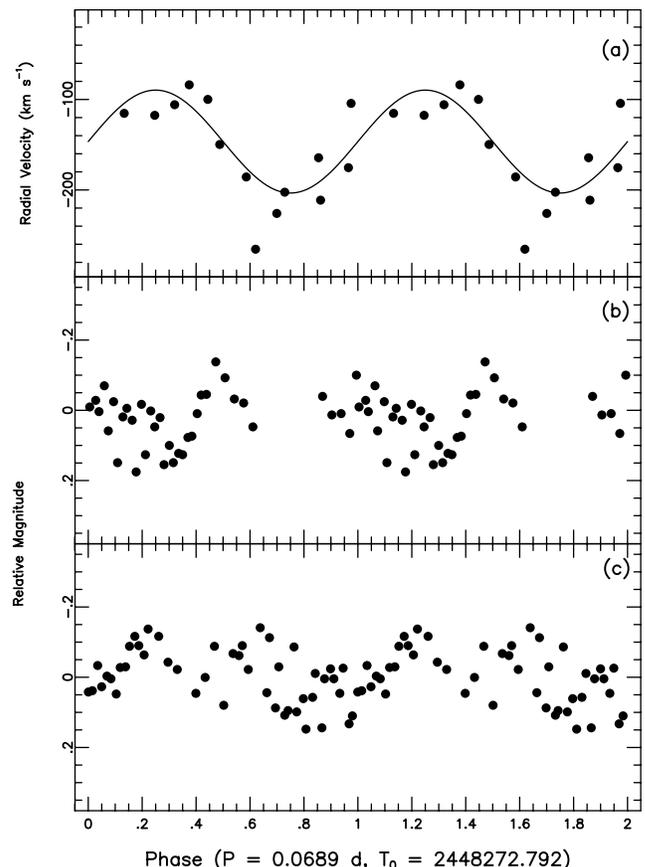

Fig. 10.—(a) Hβ radial velocities obtained on 1991 January 16 and (b, c) V-band CCD photometry obtained on the nights of 1991 January 15 and 16, respectively, folded on the best-fit spectroscopic period. The solid line is the best-fitting sinusoid, with a semiamplitude of 57 km s^{-1}. The rms error of the velocity points with respect to the curve is 32 km s^{-1}.

TABLE 1

Hα RADIAL VELOCITIES

HJD[a]	V (km s^{-1})	HJD[a]	V (km s^{-1})	HJD[a]	V (km s^{-1})	HJD[a]	V (km s^{-1})
178.8350......	−42	179.6856......	4	181.7789......	−21	181.9160......	−17
178.8411......	−67	179.6916......	13	181.7850......	−24	181.9221......	19
178.8471......	−85	179.6977......	0	181.8708......	−118	181.9281......	−57
178.8532......	−132	179.7037......	35	181.8769......	−106	181.9342......	−106
178.8592......	−88	180.8592......	−120	181.8830......	−134	182.6331......	−152
178.8653......	−102	180.8713......	−104	181.8891......	−72	182.6495......	−34
178.8813......	−22	180.8773......	−118	181.8951......	−53	182.6556......	−125
178.8934......	12	181.7662......	−9	181.9038......	−19	182.6761......	−106
179.6796......	−43	181.7722......	−39	181.9099......	−18	182.6821......	−162

[a] Heliocentric JD of mid-integration minus 2,450,000.

0.5 in phase. These data indicate that the light curve changes on relatively short timescales and that the cusp was a transitory event and not typical of every orbital cycle.

To improve the accuracy of the orbital period derived from photometry and limited MMT spectroscopy, we observed SX LMi on five bright or gray nights in 1996 April with the MDM 2.4 m Hiltner Telescope. The instrumental setup and average spectrum were discussed in § 4. SX LMi appeared to be at minimum light. The seeing and transparency were often poor and some of the spectra were unusable, so we reviewed the 52 integrations of 8 minutes' length individually, rejecting 14 for insufficient signal-to-noise ratio. The remaining spectra spanned 7.2 hr of hour angle. Simultaneous photometry was not obtained.

We measured Hα velocities (Table 1) with the double-Gaussian convolution technique described earlier. The Gaussian separation used was 1740 km s^{-1}, again similar to our earlier measures. The period search of these velocities, shown in Figure 11, uses a "residual gram" technique, explained by Thorstensen et al. (1996); it selects a most likely period near 0.06717 days (14.89 cycles day^{-1}). Because of the limited signal-to-noise ratio of the velocities, daily cycle-count aliases at 0.07187 days (13.91 cycles day^{-1}) and 0.06298 days (15.88 cycles day^{-1}) are stronger than one would prefer. To determine the confidence with which we could identify the best-fitting alias with the true period, we used the Monte Carlo test of Thorstensen & Freed (1985).

We tested one alias against an alternative, and for the standard deviation of the artificial data we used the scatter around one of the alternate periods in the actual data. This yielded a (one-sided) discriminatory power of 966/1000 and a correctness likelihood of 315/316; a two-sided test would reduce these to about 932/1000 and 314/316. Thus the
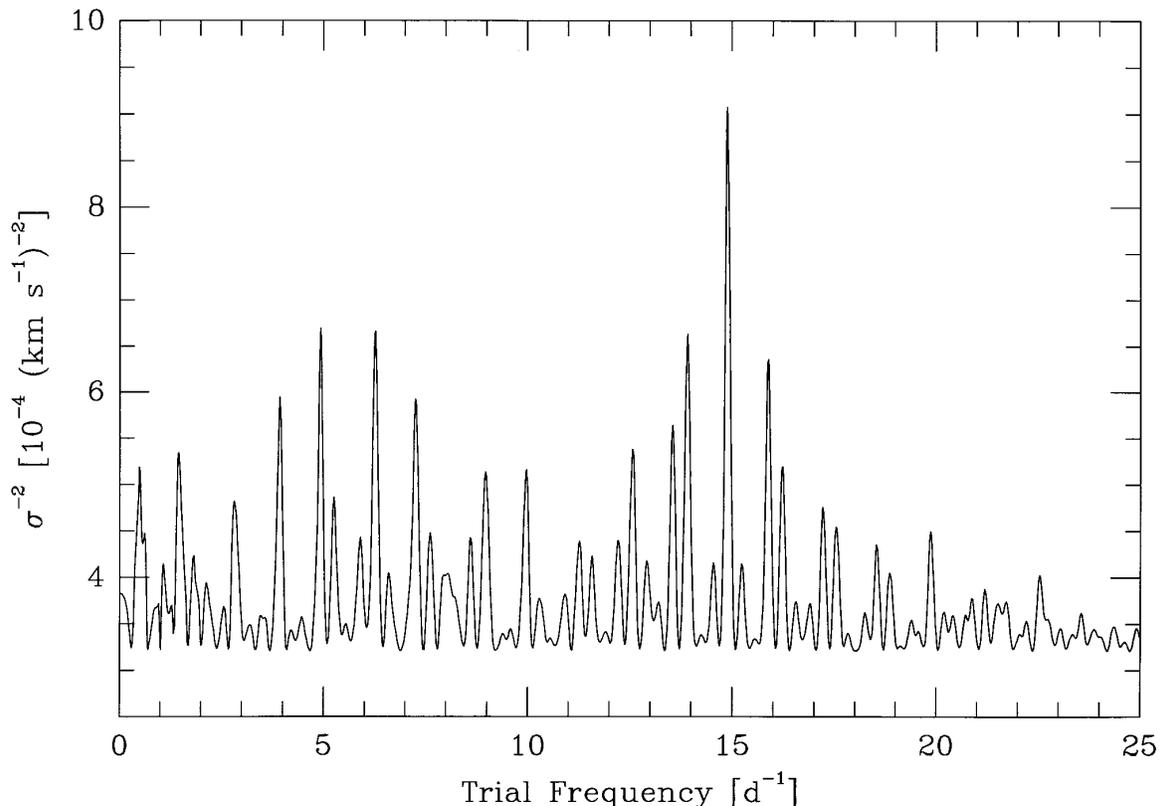

FIG. 11.—Periodogram of the MDM Hα radial velocities computed as the inverse square of the sinusoid fit residuals. The highest peak corresponds to the adopted period.
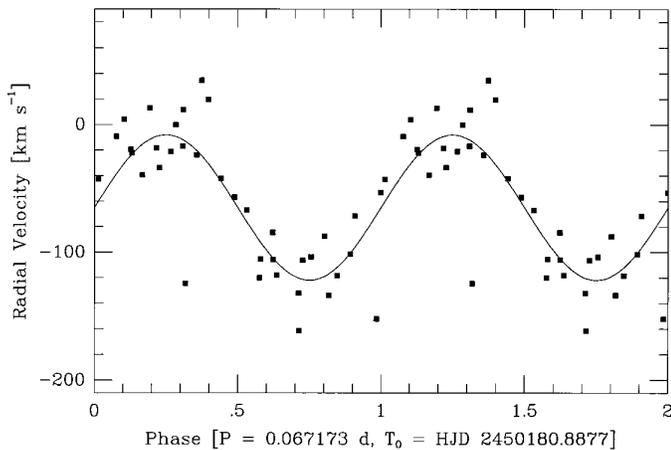
FIG. 12.—MDM radial velocities of the Hα line, folded on the adopted period. All data are plotted twice for continuity. The best-fitting sinusoid, with a period of 0.067173 days and a semiamplitude of 57 km s^{-1}, is plotted as a solid line. The rms error of the solution is 34 km s^{-1}.

alias choice is reasonably secure, but not completely definitive. The best-fit sinusoid had

$$T_0 = \text{HJD } 2,450,180.8877 \pm 0.0021 ,$$

$$P = 0.06717 \pm 0.00011 \text{ days} ,$$

$$K = 57 \pm 10 \text{ km s}^{-1} ,$$

$$\gamma = -65 \pm 7 \text{ km s}^{-1} ,$$

$$\sigma = 33.7 \text{ km s}^{-1} .$$

This sinusoid is superposed on the folded Hα radial velocities in Figure 12. As with the MMT velocities, there are significant deviations from the best fit, which tend to occur at the extrema of the velocity curve near phases 0.25 and 0.75. Surprisingly, the semiamplitude K from the MDM data is essentially identical to that obtained from the MMT spectra, but the systemic velocities differ considerably. Such a difference could result from a time-dependent outflow or wind from the accretion disk.

7. OUTBURST OBSERVATIONS

On 1994 December 13, an outburst of SX LMi was discovered by RoboScope. At the time of the discovery, SX LMi had reached $V = 13.43$, rising from its quiescence at $V \simeq 17.4$ and implying an outburst amplitude of at least 4 mag, since RoboScope did not monitor the entire outburst. The data do not resolve the onset of the outburst, since the previous measurement was obtained 11 days earlier, when SX LMi was at $V = 17.51$. Likewise, the end of the outburst was not resolved since the next measurement was obtained on December 26, when the star had faded to $V = 16.72$. Evidently, the outburst ended sometime between December 22 and 26, since we observed superhumps on December 22 (see below).

Alerted to the outburst by RoboScope, we obtained time series differential photometry on the nights of 1994 December 20, 21, and 22, using the National Undergraduate Research Observatory (NURO) 0.8 m telescope at the Lowell Observatory and the NURO direct-imaging CCD camera. The camera consists of a filter wheel and a Tektron-

ix thinned back-illuminated 512^2 CCD yielding ~0″.45 pixel^{-1}. The seeing was typically 2″–2″.5, and integration times were 300 s with 30 s of dead time between exposures. On December 20, we obtained photometry through a Johnson B filter for 2.73 hr. On December 21 and 22, we used a Johnson V filter for durations of 2.73 and 3.44 hr, respectively. Bias and flat-field frames were obtained on each night, but absolute calibration was not attempted.

Figure 13 shows the outburst light curves. The obvious superhumps confirm the membership of SX LMi in the SU UMa subclass. In general, superhumps should decline in intensity to shorter wavelengths since their source is rather cool (Hassall 1985; Naylor et al. 1988), but must have a rather large emitting area at the edge of the accretion disk to account for their great strength (Naylor et al. 1988). The superhumps on December 21 are triangular in shape but may be more rounded one night later, on December 22. This behavior is consistent with other SU UMa systems, such as Z Cha (Warner & O'Donoghue 1988), in which the superhumps have large amplitude and are triangular in profile at the beginning of the outburst but become more rounded and of lower amplitude later in the outburst.

To determine a superhump period, we began by fitting ~0.068 day sinusoids to the individual nights' data and
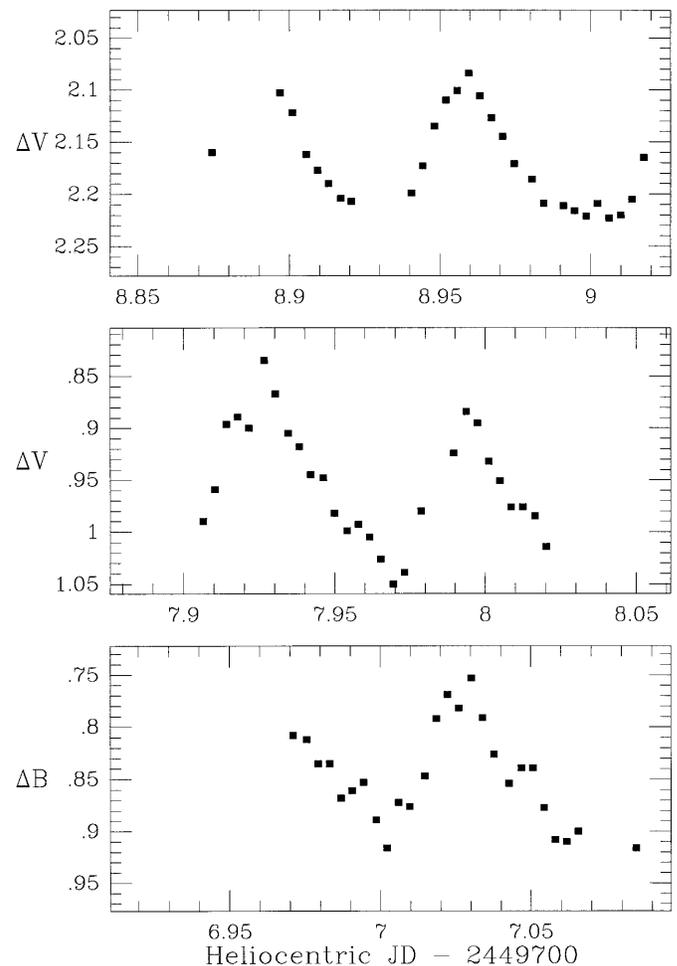

FIG. 13.—Differential photometry of SX LMi obtained during the 1994 December superoutburst at NURO. The horizontal scale for each night is the same, but the starting times of the plots have been arranged so that the superhumps line up from night to night. A period of 0.06893 days was assumed for this alignment.

adjusting the different nights to a common mean of zero; we then searched for periods in the merged, adjusted time series using the "residual gram" technique (Thorstensen et al. 1996). Although this technique formally assumes the data to be sinusoidal, it is sensitive to quasi-sinusoidal variations like those seen here. Figure 14 shows the result; a frequency near 14.51 cycles day^{-1} is strongest, but daily cycle-count aliases are also present. The aliasing results from the modest range of hour angle spanned by the observations (inevitable in view of its right ascension and the time of year the outburst occurred). The best alias corresponds to a superhump period $P_{SH} = 0.06893 \pm 0.00012$ days, which, as expected, is a little longer than the orbital period found above, $P_{orb} = 0.06717$ days. Although the superhump data do not carry much weight in the choice of daily cycle-count alias, they are nicely consistent with our preferred spectroscopic period and do give us some extra confidence that we chose the correct spectroscopic period.

The SU UMa stars show a correlation between P_{orb} and the superhump period excess $\epsilon = (P_{SH} - P_{orb})/P_{orb}$. Thorstensen et al. (1996) recently revisited this correlation and found the mean relation

$$\epsilon = -0.0344 + (0.0382 \text{ hr}^{-1})P_{orb} .$$

For SX LMi this relation predicts $\epsilon = 0.027$, and we observe $\epsilon = 0.026 \pm 0.002$, which is just as expected.

During the 1994 December superoutburst of SX LMi, we also obtained several low-dispersion spectra using the Steward Observatory CCD spectropolarimeter (SPOL; Schmidt, Stockman, & Smith 1992) in its nonpolarimetric mode on the Perkins Telescope. Spectra obtained on 1994

December 18, 19, 21, and 27 are shown in Figure 15. The red spectra, obtained December 18 and 19, cover 5500–8050 Å; those obtained December 21 and 27 cover 4500–7000 Å. SPOL utilizes a thinned back-illuminated Loral 1200 × 800 CCD and a 1200 groove mm^{-1} grating. When combined with a 5″ entrance slit, it yields a spectral resolution ∼6 Å. The seeing was typically 2″–2″.5. For wavelength calibration we used spectra of HgNeXe lamps, and the spectrum of an illuminated white screen was used as a flat field. We used EG 184 as a standard for relative flux calibration.

The December 18 and 19 (red) spectra show Hα and He I λ6678 and λ7065 emission lines superposed on a relatively steep blue continuum. The measured equivalent width and FWHM for Hα on both December 18 and 19 are respectively 7 Å and 1000 km s^{-1}. During quiescence, the equivalent width of Hα is ∼83 Å, so much of the decrease in its equivalent width can be explained by the brightening of the continuum during the outburst. Bluer spectra on December 21 show emission not only at Hα but also at Hβ, superposed on a broad absorption profile. On December 21 the net equivalent width and FWHM of the Hα emission were respectively 8 Å and 926 km s^{-1}, comparable to the previous days. By December 27, the outburst had subsided and the spectrum was similar to the quiescent spectra. The equivalent widths of Hα and Hβ emission were 62 and 51 Å, respectively.

The December 18 spectra span about 1 hr, or nearly two-thirds of the orbital period. There are six spectra with 600 s integration times. Figure 16 shows the Hα profiles for each of the six spectra. Note the dramatic profile variations on timescales of ∼10 minutes. When the sequence begins,
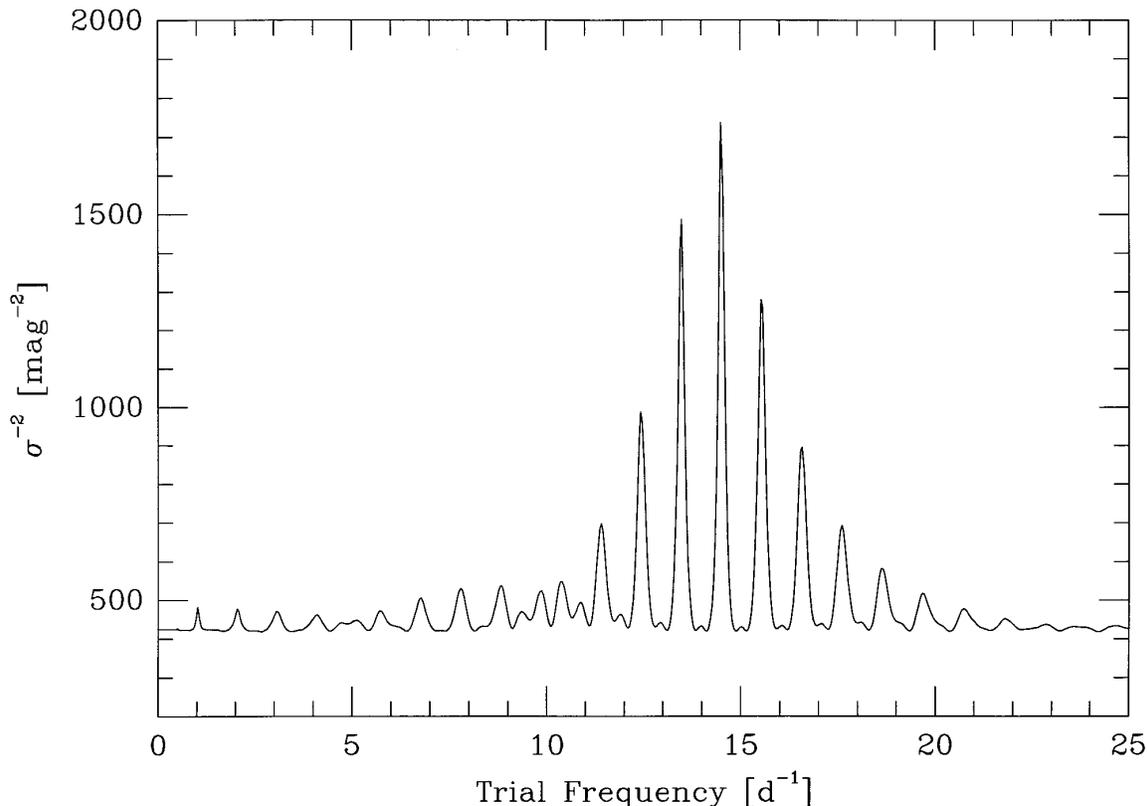

Fig. 14.—Period search of the superhump photometry, computed as described in the text. The highest peak indicates the derived superhump period of 0.06893 ± 0.00012 days.
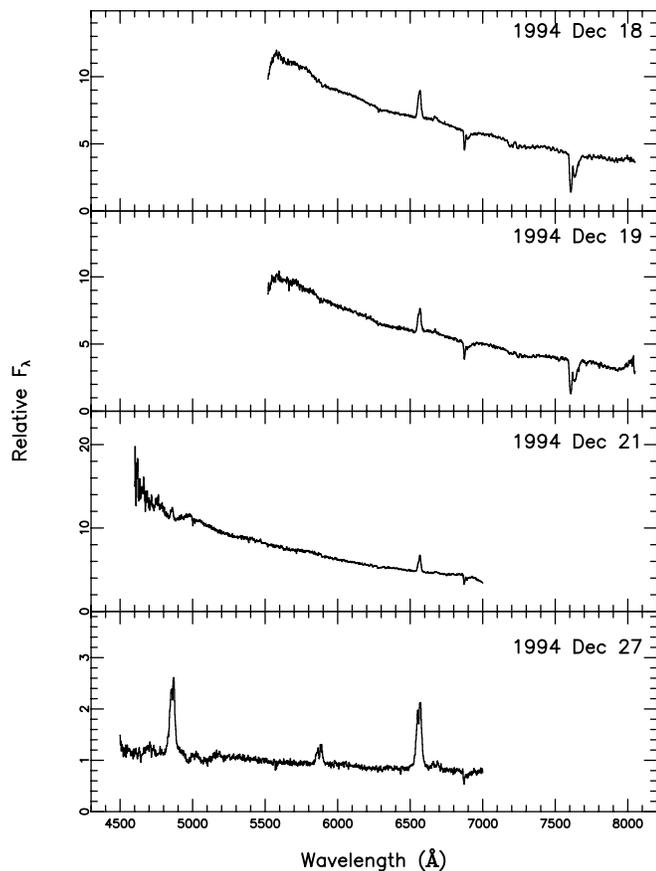
FIG. 15.—Spectra of SX LMi obtained during the 1994 December superoutburst with SPOL on the Perkins Telescope. The spectra obtained between December 18 and 21 were during the outburst, but by December 27 the outburst had ended and returned to quiescence.

the profile is highly asymmetric to the blue, but only 10 minutes later the profile is fairly symmetric and shows double peaks. In the next time step, the profile is highly asymmetric to the red. Later spectra, which encompass nearly half the orbit, show it to be relatively symmetric. Similar line-profile variations have been observed in other SU UMa systems, such as Z Cha (Vogt 1982) and SU UMa itself (Rutten et al. 1992).

The variations exhibited by the line profiles on December 18 and their diversity on December 21 led us to model their physical origin in the disk. We assume a circularly symmetric, flat, nonturbulent, geometrically thin accretion disk in Keplerian rotation. We further assume that the density distribution of the emitting atoms is a power-law function of the disk radius in which the radial coordinate r is normalized to $r = 1$ at the outer edge of the disk. The emission-line profile can then be expressed as

$$F(u) \propto \int_{r_1}^{r_z} \frac{r^{3/2} f(r) dr}{(1 - u^2 r)^{1/2}}$$

(Shakura & Sunyaev 1973; Smak 1981), where u is the dimensionless radial velocity ($u = 1$ when $r = 1$), r_1 is the ratio of the inner radius to the outer radius of the disk, $r_z = \min (1, u^{-2})$, and $f(r) \sim r^{-\alpha}$. The parameter α ranges from zero to 2.5, and the integral can be evaluated analytically for integer and half-integer values of α within this range. For line profiles that characterize cataclysmic variables, $\alpha \simeq 2$ (Smak 1981). In addition to the disk component described above, we included a Gaussian line component to represent the broad absorption component of the Hβ line profile in Figure 15 or asymmetries in the emission-line profiles, whether they are produced by additional emission or absorption lines. The disk profile and Gaussian com-
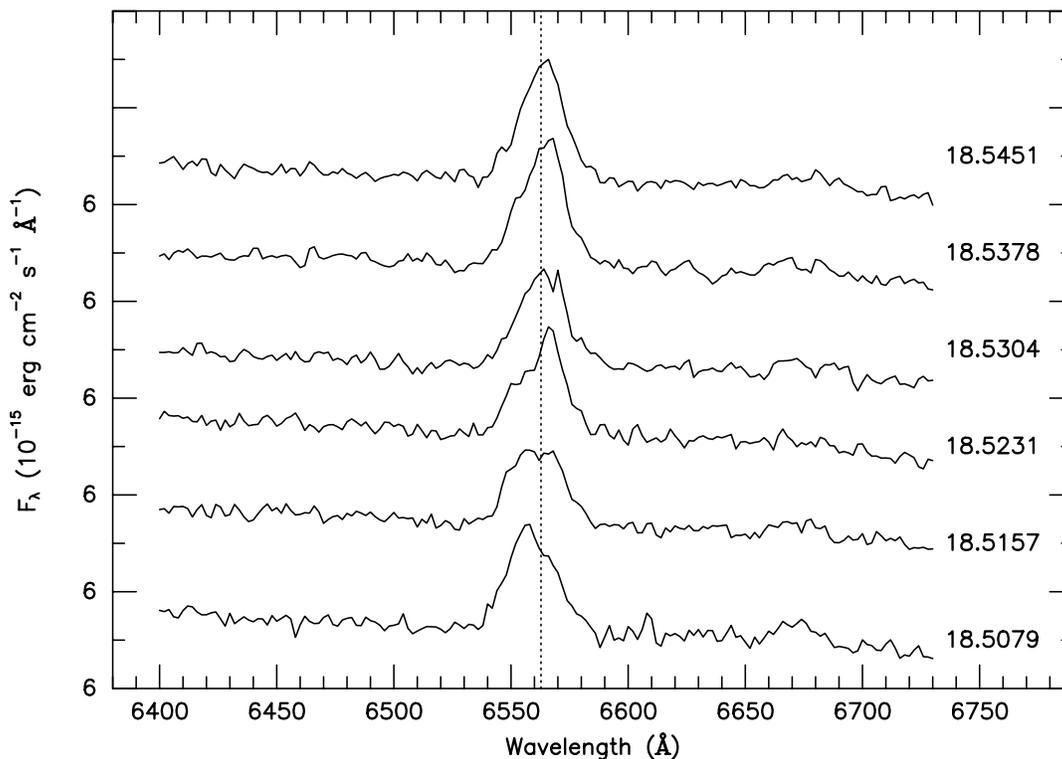

FIG. 16.—Time series spectra of SX LMi centered on the Hα emission line obtained over an hour's time span on 1994 December 18 during the superoutburst. Note the dramatic Hα line profile variations on timescales of 10 minutes. A fiducial flux is indicated for each spectrum. Each successive tick mark represents a difference of 10^{-15} ergs cm^{-2} s^{-1} Å^{-1}.

ponent superposed on a linear background continuum define our model line profile. Comparisons with the observed data were made using a nonlinear least-squares fitting program with the model profile and evaluated at each step using a χ^2 statistic.

The results for the December 21 Hα and Hβ line profiles are shown in the top and bottom panels of Figure 17, respectively. The crosses represent the data, and the final fit and individual profile components are respectively shown as heavy solid lines and dotted lines. The observed Hα profile is highly asymmetric to the red. We found that this profile could be best represented by an accretion disk profile and a slightly blueshifted narrow absorption line. The disk profile is characterized by $\alpha = 2$, which yielded the best-fit solution with respect to the data for integer and half-integer values of α between zero and 2.5. We find that the ratio of the inner edge of the disk to the outer edge is $r_1 = 0.03$ and that the velocity at the outer edge of the disk, u_2, is about 152 km s^{-1}. The equivalent width of the disk component is 11.4 Å. The absorption line is blueshifted with respect to the emission-line component by -110 km s^{-1}, and its equivalent width is 2.3 Å. The half-width of the absorption line is about 274 km s^{-1}.

These results can be compared with those for Hβ, in which we might naively expect the disk parameters to be similar to those derived from the Hα profile. The signal-to-noise ratio of the Hβ profile is not nearly as good as that of Hα, and its profile is complicated by the presence of a broad

absorption component. As for Hα, we find that the best-fit solution yields $\alpha = 2$. We find, for the disk component arising from Hβ, that $r_1 = 0.05$ and $u_2 = 271$ km s^{-1} and that its equivalent width is 2.7 Å. The systemic velocities of Hα and Hβ emission derived from our fitting are quite different, -68 and -351 km s^{-1} for Hα and Hβ, respectively. The broad absorption component of Hβ is characterized by a half-width of 5200 km s^{-1} and an equivalent width of 9 Å.

The deblended emission-line intensities of Hα and Hβ, compared with those predicted from theoretical models of hydrogen emission at moderate to high densities, allow us to infer some physical characteristics of the accretion disk in outburst. The observed Hα/Hβ intensity ratio is 1.7 and when corrected for the small amount of reddening will be slightly flatter. Comparison with the models presented by Drake & Ulrich (1980) indicates that the electron temperature in the Balmer line emission region must be in excess of $\simeq 5000$ K. At a temperature of 5000 K, the Hα/Hβ ratio is never less than about 2.4 over a wide range of Hα and Lyα optical depths. It is also clear that the Hα optical depth must be large given the relatively flat decrement, since the Hα/Hβ ratio tends to unity at large optical depths. For a temperature of 10^4 K and $\tau(\text{H}\alpha) \gtrsim 10$, then $\log N_e(\text{cm}^{-3}) \gtrsim 12.5$ in the Balmer line region. The decrement does not place an upper limit on the temperature in the Balmer line region.

Our constraints on the temperature derived from the emission lines compare favorably to those inferred based on the wavelength dependence of the superhump amplitudes (Hassall 1985; Naylor et al. 1988), in which $T = 6000$–10,000 K. The physical situation might well be described by an accretion disk with $T \simeq 7500$–10,000 K, $\log N_e \simeq 13$, and large Lyα and Hα optical depths.

8. DISCUSSION

We have shown that SX LMi is an SU Ursae Majoris star with an orbital period near 97 minutes and a superhump period excess typical of other SU UMa stars with similar orbital periods. We can estimate the distance to SX LMi by using Warner's (1987) relationship between minimum absolute magnitude and orbital period, $M_V(\text{min}) = (9.72 \pm 0.25) - (0.337 \pm 0.056)P$, where the orbital period P is expressed in hours. For SX LMi this relation yields $M_V(\text{min}) = 9.2 \pm 0.3$ mag. Taking $V_{\min} = 17.4$ from the RoboScope results, we derive a distance of 360 pc, assuming that $A_V = 0.4$ mag ($b = 64°2$). Alternatively, we can estimate the distance to SX LMi from Warner's (1987) relationship between absolute magnitude at maximum and orbital period, $M_V(\text{max}) = (5.64 \pm 0.13) - (0.259 \pm 0.024)P$. In this case, we find that $M_V(\text{max}) = 5.2$ mag, assuming our best-fit orbital period. If $V \simeq 13.4$ at maximum, as measured by RoboScope, then we find that $d = 360$ pc, in excellent agreement with the distance derived from its orbital period and magnitude in quiescence. Since the amount of interstellar absorption in the direction of SX LMi is uncertain, an upper limit on its distance is $\simeq 440$ pc. Sproats, Howell, & Mason (1996) have placed constraints on the distance to SX LMi based on infrared magnitudes and colors and find that $d \geq 150$ pc. The implied z-distance is 330 pc, which places SX LMi considerably above the ~ 150 pc scale height of disk CVs (Patterson 1984).

The relatively small radial velocity semiamplitude and the small photometric fluctuations (± 0.18 mag) both suggest that SX LMi has a low orbital inclination. Simulta-
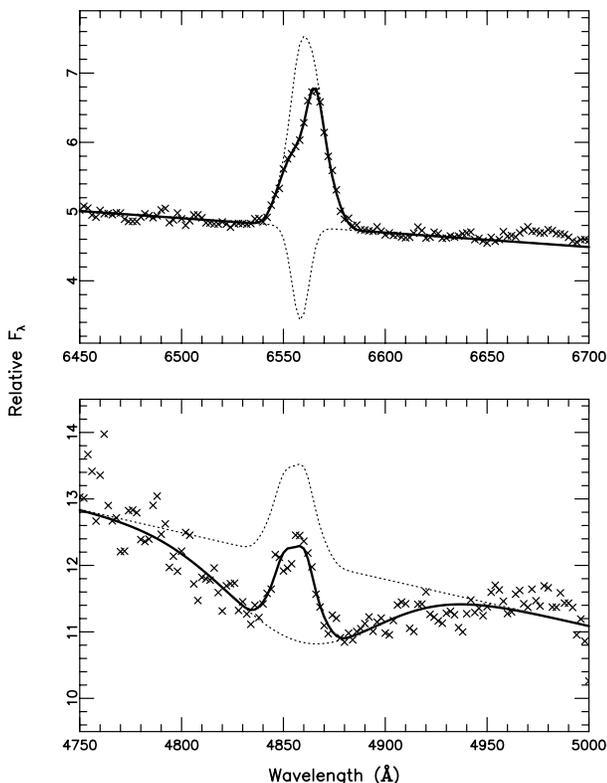

FIG. 17.—Model fitting of the Hα (top) and Hβ (bottom) line profiles during the superoutburst of SX LMi on 1994 December 21. The data are represented by crosses. The individual line components are shown as dotted lines. The final fit is shown as the heavy solid line. The Hα line profile consists of a disk component superposed with a narrow and slightly blueshifted absorption line. The Hβ line consists of a disk component superposed with a broad absorption line.

neous photometry and spectroscopy allow the unambiguous phasing of the light curve with respect to the velocities, as shown in Figure 10, and there is no indication that a bright spot dominates the light curve or that a strong S-wave component dominates the H line profiles in SX LMi. In most nova-like CVs, there is little or no evidence that a bright spot contributes to the emission-line profiles (Warner 1995 and references therein) in these high accretion rate systems. This comparison suggests that SX LMi probably has a relatively high accretion rate for a typical SU UMa system below the period gap. This behavior contrasts with other SU UMa systems (Osaki 1996 and references therein), which are believed to have mass accretion rates of 10^{16} g s^{-1} or less. There is no evidence that SX LMi is a member of the "ER UMa stars" or "RZ LMi stars" (Kato & Kunjaya 1995; Robertson, Honeycutt, & Turner 1995), which constitute an extreme group of SU UMa stars characterized by short supercycles (20–45 days) and frequent normal outbursts ($\sim$4 days). Modeling (Osaki 1996 and references therein) indicates that these systems have accretion rates well in excess of 10^{16} g s^{-1}, in contrast to normal SU UMa systems. SX LMi may have an accretion rate intermediate between these two classes of SU UMa stars. The correspondingly higher disk luminosity in SX LMi prevents detection of the secondary star in the red portions of our optical spectra and in the infrared (Sproats et al. 1996).

Long-term RoboScope monitoring shows that SX LMi undergoes outbursts at intervals of 34–64 days with a mean amplitude of about 3.5 mag, but the duration of the outbursts is not well constrained since there are significant gaps in our coverage. At the time of one of these outbursts (1994 December) superhumps were observed in the light curve, indicating at least one superoutburst of the system between late 1992 and mid-1995. Superoutbursts generally last longer than ordinary outbursts by factors of 5–10 (Warner 1995 and references therein), but this effect is not evident in the long-term light curve of SX LMi (Fig. 2). For SU UMa stars, the observed ratio of recurrence times of superoutbursts to normal outbursts lies in the range 1–14 (Warner 1995). For example, Z Cha undergoes ordinary outbursts every $\simeq$90 days and superoutbursts every $\simeq$280 days (Bateson 1978). Observations of SU UMa over a 60-night campaign between 1988 December and 1989 January (Jones et al. 1990; Rutten et al. 1992) indicated four normal outbursts but no superoutbursts. The amplitude of these outbursts was typically $\simeq$2.5 mag. In general, SU UMa exhibits normal outbursts with recurrence times between 5 and 33 days (Casares, Charles, & van Paradijs 1990). For SX LMi, the data suggest that the superoutburst period must be less than $\sim$170 days. If normal outbursts occur at intervals of 34–64 days, then the outbursting behavior of SX LMi is similar to other SU UMa systems. A periodogram of the quiescent RoboScope data in the range 0.065–0.070 days, and thus covering the orbital period, did not indicate the presence of any statistically significant periodicities.

The spectrum of SX LMi in quiescence is similar to that of other dwarf novae (DNs) in their low states (Warner 1995). These spectra are characterized by strong Balmer emission lines superposed on a blue continuum. Weaker emission lines arising from He I and, perhaps, heavier elements are also present. Emission arising from He II λ4686 and the C III/N III blend at 4650 Å is weak or absent. Fewer spectroscopic observations are available in the literature of DNs in outburst or SU UMa systems in superoutburst, as compared with photometric observations. However, our spectra of SX LMi in superoutburst are similar to those of other DNs and SU UMa systems in outburst or superoutburst. The strong Balmer emission lines that characterize their spectra in quiescence are replaced by broad and strong absorption troughs superposed on an increasingly stronger continuum. In most DNs at maximum light, weak emission-line cores are visible at the bottom of the absorption troughs. In many DNs and SU UMa systems, Hα is primarily in emission and the higher order Balmer lines are in absorption with weak emission cores because the Balmer decrement is steeper in the emission than the absorption lines (Warner 1995). In high-inclination systems such as Z Cha and OY Car, the spectrum consists of emission lines with narrow absorption cores (see Warner 1995 and references therein). Unpublished spectra of SU UMa and YZ Cnc obtained by Harlaftis (1992), which document in detail the spectroscopic evolution of these systems from quiescence to superoutburst and back to quiescence, bear a striking resemblance to our superoutburst spectra of SX LMi.

9. SUMMARY

1. Time-resolved spectroscopy of SX LMi in quiescence reveals radial velocity variations of the Balmer emission lines on a period of 96.72 minutes with a semiamplitude of 57 km s^{-1}. The quiescent optical spectrum of SX LMi is similar to other quiescent dwarf novae.

2. SX LMi is a member of the SU Ursae Majoris class of cataclysmic variables. Photometric observations during the outburst of 1994 December show that SX LMi exhibits superhumps with a period 2.6% longer than the orbital period, as expected for a normal SU UMa system at this orbital period.

3. Long-term photometric monitoring of SX LMi by RoboScope between 1992 October and 1995 June shows seven well-defined outbursts with a mean amplitude of 3.5 mag. The outburst interval varies between 34 and 64 days. The presence of superhumps in 1994 December indicates that at least one of the outbursts discovered by RoboScope was a superoutburst.

4. The spectrum of SX LMi in superoutburst is similar to those of other dwarf novae in outburst or superoutburst. Spectra obtained during superoutburst show dramatic variations in the emission-line profiles on timescales of less than 10 minutes. Analysis of the average line profiles in superoutburst indicates that underlying absorption contributes to the shape of the Balmer line profiles. The Balmer decrement during superoutburst constrains the temperature of the disk to be greater than 5000 K. This is consistent with the color dependence of the superhump amplitude based on observations of other systems, which declines to shorter wavelengths, and suggests $T = 6000$–$10,000$ K.

REFERENCES

Bateson, F. M. 1978, MNRAS, 184, 567
Casares, J., Charles, P. A., & van Paradijs, J. 1990, in Accretion-powered Compact Binaries, ed. C. W. Mauche (Cambridge: Cambridge Univ. Press), 101
Drake, S. A., & Ulrich, R. K. 1980, ApJS, 42, 351
Harlaftis, E. T. 1992, Ph.D. thesis, Univ. Oxford
Hassall, B. J. M. 1985, MNRAS, 216, 335
Henden, A. A., & Honeycutt, R. K. 1995, PASP, 107, 324
Honeycutt, R. K. 1992, PASP, 104, 435
Honeycutt, R. K., & Turner, G. W. 1992, in ASP Conf. Ser. 34, Robotic Telescopes in the 1990s, ed. A. V. Filippenko (San Francisco: ASP), 77
Honeycutt, R. K., Vesper, D. N., White, J. C., Turner, G. W., & Adams, B. R. 1990, in CCDs in Astronomy II, ed. A. G. D. Philip & D. S. Hayes (Schenectady: L. Davis), 177
Howell, S. B., Mitchell, K. J., & Warnock, A. 1988, AJ, 95, 247
Jones, D. H. P., et al. 1990, in Accretion-powered Compact Binaries, ed. C. W. Mauche (Cambridge: Cambridge Univ. Press), 97
Kato, T., & Kunjaya, C. 1995, PASJ, 47, 163
Molnar, L. A., & Kobulnicky, H. A. 1992, ApJ, 392, 678
Naylor, T., Bath, G. T., Charles, P. A., Hassall, B. J. M., Sonneborn, G., van der Woerd, H., & van Paradijs, J. 1988, MNRAS, 231, 237
Osaki, Y. 1996, PASP, 108, 39
Patterson, J. 1984, ApJS, 54, 443

Robertson, J. W., Honeycutt, R. K., & Turner, G. W. 1995, PASP, 107, 443
Rutten, R. G. M., et al. 1992, in ASP Conf. Ser. 29, Cataclysmic Variable Stars, ed. N. Vogt (San Francisco: ASP), 148
Sanduleak, N., & Pesch, P. 1984, ApJS, 55, 517 (erratum 103, 513 [1996])
Schmidt, G. D., Stockman, P. S., & Smith, P. S. 1992, ApJ, 398, L57
Schneider, D. P., & Young, P. 1980, ApJ, 238, 946
Shafter, A. W. 1983, ApJ, 267, 222
Shafter, A. W., & Szkody, P. 1984, ApJ, 276, 305
Shakura, N. I., & Sunyaev, R. A. 1973, A&A, 24, 337
Smak, J. 1981, Acta Astron., 31, 395
Sproats, L. N., Howell, S. B., & Mason, K. O. 1996, MNRAS, 282, 1211
Stellingwerf, R. F. 1978, ApJ, 224, 953
Szkody, P., & Howell, S. B. 1992, ApJS, 78, 537
Thorstensen, J. R., & Freed, I. B. 1985, AJ, 90, 2082
Thorstensen, J. R., Patterson, J., Thomas, G., & Shambrook, A. 1996, PASP, 108, 73
Vogt, N. 1982, ApJ, 252, 653
Wagner, R. M., Sion, E. M., Liebert, J., & Starrfield, S. G. 1988, ApJ, 328, 213
Warner, B. 1987, MNRAS, 227, 23
———. 1995, Cataclysmic Variable Stars (Cambridge: Cambridge Univ. Press)
Warner, B., & O'Donoghue, D. 1988, MNRAS, 233, 705

NOTE ADDED IN PROOF.—Photometric observations of SX LMi during its 1994 superoutburst and their interpretation by D. Nogami, S. Masuda, & T. Kato (PASP, 109, 1114 [1997]) are consistent with the results presented here although their superhump period ($P = 0.06950 \pm 0.00002$ days) is slightly longer than our value.